LTH 628
CERN-PH-TH/2004-153
hep-ph/0408128

Snowmass Benchmark Points and Three-Loop Running

I. Jack, D.R.T. Jones[1] and A.F. Kord

Department of Mathematical Sciences, University of Liverpool, Liverpool L69 3BX, U.K.

We present the full three-loop β-functions for the MSSM generalised to include additional matter multiplets in 5, 10 representations of SU(5). We analyse the effect of three-loop running on the sparticle spectrum for the MSSM Snowmass Benchmark Points. We also consider the effect on these spectra of additional matter multiplets (the semi-perturbative unification scenario).

August 2004

[1] address from Sept 1st 2003- 31 Aug 2004: TH Division, CERN, 1211 Geneva 23, Switzerland

1. Introduction

The LHC will soon resolve the question as to whether low energy supersymmetry is the solution to the hierarchy problem; and if it is, moreover, the LHC and a future e^+e^- linear collider (LC) will lead to very precise measurements of the sparticle spectrum and couplings. The success of gauge unification in the MSSM suggests a Desert, the existence of which would mean that extrapolation of the MSSM couplings and masses to high scales will lead to immediate information about the underlying theory; for example regarding the commonly assumed universality of soft scalar masses, gaugino masses and cubic scalar interactions.

One component of this analysis is the running of masses and couplings between the weak and gauge unification scales, which is governed by the renormalisation group β-functions. In this paper we compare the results for this process using one, two and three-loop β-functions. In each case we generally use the same one-loop corrections for the relationship between running and pole masses for the various particles, with some use of two-loop results such as for the top quark mass. We anticipate that by the time sparticles are discovered complete two-loop threshold corrections will be available; the effect of these we would expect to be of the same order of magnitude as the effect of using the three-loop (as opposed to two-loop) β-functions, which, as we shall see, is surprisingly large for squarks.

The plan of this paper is as follows. In section 2 we review the exact results that relate the β-functions for the soft masses and interactions[1] –[3] to the β-functions of the dimensionless gauge and Yukawa couplings [4]– [6], which we then give through three loops for the MSSM generalised to incorporate n_5 and n_{10} sets of SU_5 $5(\overline{5})$ and $10(\overline{10})$ representations respectively. (A motive for grouping additional matter in this way is that complete SU_5 representations do not (at one loop) change the prediction of $\sin^2\theta_W$ (or alternatively of $g_3^2(M_Z)$) that follows from imposing $g_{1,2,3}$ gauge unification. Also unchanged at one loop is the gauge unification scale, M_X; but at higher loops this scale increases and can approach the string scale.) We also give a simplified example of a three-loop soft β-function; general results for all the β-functions are available at Ref. [7].

In section 3 we present and discuss our results for the sparticle spectrum for a set of Snowmass Benchmark Points[8], all corresponding to the standard universal boundary conditions at unification, except for one case with non-universal gaugino masses. We compare our results with the useful website Ref. [9] (see also Refs. [10], [11]).

In section 4 we consider the effect of additional matter fields in SU_5 representations, as discussed in Refs. [12], [13] (for earlier work see for example Refs. [14]) and by ourselves in a previous paper [15]. We give some further examples of the effect on the sparticle spectrum of such matter. Finally section 5 contains our conclusions.

2. The Soft Beta functions

For a general $N = 1$ supersymmetric gauge theory with superpotential

$$W(\phi) = \tfrac{1}{2}\mu^{ij}\phi_i\phi_j + \tfrac{1}{6}Y^{ijk}\phi_i\phi_j\phi_k, \tag{2.1}$$

the standard soft supersymmetry-breaking scalar terms are as follows

$$V_{\rm soft} = \left(\tfrac{1}{2}b^{ij}\phi_i\phi_j + \tfrac{1}{6}h^{ijk}\phi_i\phi_j\phi_k + \text{c.c.}\right) + (m^2)^i{}_j\phi_i\phi^j, \tag{2.2}$$

where we denote $\phi^i \equiv \phi_i^*$ etc. (For the generalisation to the case when $V_{\rm soft}$ includes a term linear in ϕ see [16].)

The complete exact results for the soft β-functions are given by:

$$\begin{aligned}
\beta_M &= 2\mathcal{O}\left[\frac{\beta_g}{g}\right], \\
\beta_h^{ijk} &= h^{l(jk}\gamma^{i)}{}_l - 2Y^{l(jk}\gamma_1{}^{i)}{}_l, \\
\beta_b^{ij} &= b^{l(i}\gamma^{j)}{}_l - 2\mu^{l(i}\gamma_1{}^{j)}{}_l, \\
(\beta_{m^2})^{\,i}{}_j &= \Delta\gamma^i{}_j,
\end{aligned} \tag{2.3}$$

where γ is the matter multiplet anomalous dimension, and

$$\mathcal{O} = Mg^2\frac{\partial}{\partial g^2} - h^{lmn}\frac{\partial}{\partial Y^{lmn}}, \tag{2.4a}$$

$$(\gamma_1)^i{}_j = \mathcal{O}\gamma^i{}_j, \tag{2.4b}$$

$$\Delta = 2\mathcal{O}\mathcal{O}^* + 2MM^*g^2\frac{\partial}{\partial g^2} + \left[\tilde{Y}^{lmn}\frac{\partial}{\partial Y^{lmn}} + \text{c.c.}\right] + X\frac{\partial}{\partial g}. \tag{2.4c}$$

Here M is the gaugino mass and $\tilde{Y}^{ijk} = (m^2)^i{}_l Y^{jkl} + (m^2)^j{}_l Y^{ikl} + (m^2)^k{}_l Y^{ijl}$. Eq. (2.3) holds in a class of renormalisation schemes that includes the DRED′-one[17], which we will use throughout.

Finally the X function above is given (in the NSVZ scheme [18]) by

$$X^{\rm NSVZ} = -2\frac{g^3}{16\pi^2}\frac{S}{[1 - 2g^2C(G)(16\pi^2)^{-1}]} \tag{2.5}$$

where

$$S = r^{-1}\mathrm{tr}[m^2 C(R)] - MM^* C(G), \tag{2.6}$$

$C(R), C(G)$ being the quadratic Casimirs for the matter and adjoint representations respectively. There is no corresponding exact form for X in the DRED$'$ scheme[17]; we will require the leading and sub-leading contributions, which are given by[19]:

$$16\pi^2 X^{\mathrm{DRED}'(1)} = -2g^3 S \tag{2.7}$$

and

$$(16\pi^2)^2 X^{\mathrm{DRED}'(2)} = (2r)^{-1} g^3 \mathrm{tr}[WC(R)] - 4g^5 C(G) S - 2g^5 C(G) QMM^*, \tag{2.8}$$

where

$$\begin{aligned} W^j{}_i = &\frac{1}{2} Y_{ipq} Y^{pqn} (m^2)^j{}_n + \frac{1}{2} Y^{jpq} Y_{pqn} (m^2)^n{}_i + 2 Y_{ipq} Y^{jpr} (m^2)^q{}_r \\ &+ h_{ipq} h^{jpq} - 8 g^2 MM^* C(R)^j{}_i. \end{aligned} \tag{2.9}$$

and $Q = T(R) - 3C(G)$, and $rT(R) = \mathrm{tr}\,[C(R)]$, r being the number of group generators.

We now present the results for the gauge β-functions and anomalous dimensions. These results are valid in the DRED$'$ scheme[17] (or indeed the DRED one[20], which differs from DRED$'$ only when we come to the soft β-functions). The MSSM superpotential is:

$$W = H_2 Q Y_t t^c + H_1 Q Y_b b^c + H_1 L Y_\tau \tau^c + \mu H_1 H_2 \tag{2.10}$$

where Y_t, Y_b, Y_τ are $n_g \times n_g$ Yukawa matrices [2] , and we define

$$T = Y_t\, Y_t^\dagger, B = Y_b\, Y_b^\dagger, E = Y_\tau\, Y_\tau^\dagger, \tilde{T} = Y_t^\dagger Y_t\,, \tilde{B} = Y_b^\dagger Y_b\,, \tilde{E} = Y_\tau^\dagger Y_\tau\,. \tag{2.11}$$

The $SU_3 \otimes\ SU_2 \otimes\ U_1$ gauge β-functions are as follows:

$$\beta_{g_i} = (16\pi^2)^{-1} b_i g_i^3 + (16\pi^2)^{-2} g_i^3 \left(\sum_j b_{ij} g_j^2 - a_i \right) + (16\pi^2)^{-3} \beta_{g_i}^{(3)} + \cdots \tag{2.12}$$

where

$$\begin{aligned} &b_1 = \tfrac{1}{2} n_5 + \tfrac{3}{2} n_{10} + \tfrac{33}{5}, \quad b_2 = \tfrac{1}{2} n_5 + \tfrac{3}{2} n_{10} + 1, \quad b_3 = \tfrac{1}{2} n_5 + \tfrac{3}{2} n_{10} - 3 \\ &a_1 = \tfrac{26}{5} \mathrm{tr} T + \tfrac{14}{5} \mathrm{tr} B + \tfrac{18}{5} \mathrm{tr} E, \quad a_2 = 6\mathrm{tr} T + 6\mathrm{tr} B + 2\mathrm{tr} E, \quad a_3 = 4\mathrm{tr} T + 4\mathrm{tr} B \end{aligned} \tag{2.13}$$

[2] $Y_{t,b,\tau}$ here are the *transposes* of the Yukawa matrices used in Ref.[6].

and

$$b_{ij} = \begin{pmatrix} \frac{199}{25} + \frac{7}{30}n_5 + \frac{23}{10}n_{10} & \frac{27}{5} + \frac{9}{10}n_5 + \frac{3}{10}n_{10} & \frac{88}{5} + \frac{16}{15}n_5 + \frac{24}{5}n_{10} \\ \frac{9}{5} + \frac{3}{10}n_5 + \frac{1}{10}n_{10} & 25 + \frac{7}{2}n_5 + \frac{21}{2}n_{10} & 24 + 8n_{10} \\ \frac{11}{5} + \frac{2}{15}n_5 + \frac{3}{5}n_{10} & 9 + 3n_{10} & 14 + \frac{17}{3}n_5 + 17n_{10} \end{pmatrix}. \tag{2.14}$$

For the anomalous dimensions of the chiral superfields we have at one loop:

$$\begin{aligned} 16\pi^2\gamma_t^{(1)} &= 2\tilde{T} - \tfrac{8}{3}g_3^2 - \tfrac{8}{15}g_1^2, \\ 16\pi^2\gamma_b^{(1)} &= 2\tilde{B} - \tfrac{8}{3}g_3^2 - \tfrac{2}{15}g_1^2, \\ 16\pi^2\gamma_Q^{(1)} &= B + T - \tfrac{8}{3}g_3^2 - \tfrac{3}{2}g_2^2 - \tfrac{1}{30}g_1^2, \\ 16\pi^2\gamma_{H_2}^{(1)} &= 3\mathrm{tr}T - \tfrac{3}{2}g_2^2 - \tfrac{3}{10}g_1^2, \\ 16\pi^2\gamma_{H_1}^{(1)} &= \mathrm{tr}E + 3\mathrm{tr}B - \tfrac{3}{2}g_2^2 - \tfrac{3}{10}g_1^2, \\ 16\pi^2\gamma_L^{(1)} &= E - \tfrac{3}{2}g_2^2 - \tfrac{3}{10}g_1^2, \\ 16\pi^2\gamma_\tau^{(1)} &= 2\tilde{E} - \tfrac{6}{5}g_1^2, \end{aligned} \tag{2.15}$$

and at two loops[21]:

$$\begin{aligned} (16\pi^2)^2\gamma_t^{(2)} &= -2\tilde{T}^2 - 6(\mathrm{tr}T)\tilde{T} - 2Y_t^\dagger B Y_t \ + \left(6g_2^2 - \tfrac{2}{5}g_1^2\right)\tilde{T} \\ &\quad + (\tfrac{8}{15}b_1 + \tfrac{64}{225})g_1^4 + \tfrac{128}{45}g_1^2g_3^2 + (\tfrac{8}{3}b_3 + \tfrac{64}{9})g_3^4, && (2.16a) \\ (16\pi^2)^2\gamma_b^{(2)} &= -2\tilde{B}^2 - 6(\mathrm{tr}B)\tilde{B} - 2Y_b^\dagger T Y_b \ - 2(\mathrm{tr}E)\tilde{B} + \left(6g_2^2 + \tfrac{2}{5}g_1^2\right)\tilde{B} \\ &\quad + (\tfrac{2}{15}b_1 + \tfrac{4}{225})g_1^4 + \tfrac{32}{45}g_1^2g_3^2 + (\tfrac{8}{3}b_3 + \tfrac{64}{9})g_3^4, && (2.16b) \\ (16\pi^2)^2\gamma_Q^{(2)} &= -2T^2 - 3(\mathrm{tr}T)T - 2B^2 - 3(\mathrm{tr}B)B \\ &\quad - (\mathrm{tr}E)B + g_1^2(\tfrac{4}{5}T + \tfrac{2}{5}B) + \tfrac{1}{10}g_1^2g_2^2 + 8g_3^2g_2^2 + \tfrac{8}{45}g_1^2g_3^2 \\ &\quad + (\tfrac{8}{3}b_3 + \tfrac{64}{9})g_3^4 + (\tfrac{3}{2}b_2 + \tfrac{9}{4})g_2^4 + (\tfrac{1}{30}b_1 + \tfrac{1}{900})g_1^4, && (2.16c) \\ (16\pi^2)^2\gamma_{H_2}^{(2)} &= -9\mathrm{tr}T^2 - 3\mathrm{tr}BT + \left(16g_3^2 + \tfrac{4}{5}g_1^2\right)\mathrm{tr}T + (\tfrac{3}{2}b_2 + \tfrac{9}{4})g_2^4 \\ &\quad + \tfrac{9}{10}g_1^2g_2^2 + (\tfrac{3}{10}b_1 + \tfrac{9}{100})g_1^4, && (2.16d) \\ (16\pi^2)^2\gamma_{H_1}^{(2)} &= -9\mathrm{tr}B^2 - 3\mathrm{tr}BT - 3(\mathrm{tr}E^2) + \left(16g_3^2 - \tfrac{2}{5}g_1^2\right)\mathrm{tr}B + \tfrac{6}{5}g_1^2\mathrm{tr}E \\ &\quad + (\tfrac{3}{2}b_2 + \tfrac{9}{4})g_2^4 + \tfrac{9}{10}g_1^2g_2^2 + (\tfrac{3}{10}b_1 + \tfrac{9}{100})g_1^4, && (2.16e) \\ (16\pi^2)^2\gamma_L^{(2)} &= -2E^2 - E(3\mathrm{tr}B + \mathrm{tr}E - \tfrac{6}{5}g_1^2) + (\tfrac{3}{2}b_2 + \tfrac{9}{4})g_2^4 \\ &\quad + \tfrac{9}{10}g_1^2g_2^2 + (\tfrac{3}{10}b_1 + \tfrac{9}{100})g_1^4, && (2.16f) \\ (16\pi^2)^2\gamma_\tau^{(2)} &= -2\tilde{E}^2 - \tilde{E}(6\mathrm{tr}B + 2\mathrm{tr}E - 6g_2^2 + \tfrac{6}{5}g_1^2) + (\tfrac{6}{5}b_1 + \tfrac{36}{25})g_1^4. && (2.16g) \end{aligned}$$

The three-loop gauge β-function terms are (henceforth we suppress $(16\pi^2)^{-L}$ factors).

$$\begin{aligned}
\beta_{g_1}^{(3)} =& g_1^3\Big[\tfrac{84}{5}\mathrm{tr}T^2 + 18(\mathrm{tr}T)^2 + \tfrac{54}{5}\mathrm{tr}B^2 + \tfrac{36}{5}(\mathrm{tr}B)^2 + \tfrac{58}{5}\mathrm{tr}TB + \tfrac{54}{5}\mathrm{tr}E^2 + \tfrac{24}{5}(\mathrm{tr}E)^2 \\
&+ \tfrac{84}{5}\mathrm{tr}E\mathrm{tr}B - \left(\tfrac{169}{75}g_1^2 + \tfrac{87}{5}g_2^2 + \tfrac{352}{15}g_3^2\right)\mathrm{tr}T - \left(\tfrac{49}{75}g_1^2 + \tfrac{33}{5}g_2^2 + \tfrac{256}{15}g_3^2\right)\mathrm{tr}B \\
&- (\tfrac{81}{25}g_1^2 + \tfrac{63}{5}g_2^2)\mathrm{tr}E + (\tfrac{484}{15} - \tfrac{4}{5}n_5^2 - (\tfrac{506}{45} + 6n_{10})n_5 - \tfrac{154}{5}n_{10} - \tfrac{54}{5}n_{10}^2)g_3^4 \\
&- [(\tfrac{24}{5} + \tfrac{8}{5}n_{10})g_2^2 + (\tfrac{64}{225}n_5 + \tfrac{344}{75}n_{10} + \tfrac{1096}{75})g_1^2]g_3^2 \\
&- (\tfrac{27}{40}n_5^2 + (\tfrac{27}{4} + \tfrac{9}{4}n_{10})n_5 + \tfrac{81}{5} + \tfrac{261}{20}n_{10} + \tfrac{27}{40}n_{10}^2)g_2^4 - (\tfrac{1}{50}n_{10} + \tfrac{27}{50}n_5 + \tfrac{69}{25})g_1^2g_2^2 \\
&- (\tfrac{7}{40}n_5^2 + (\tfrac{7507}{900} + \tfrac{9}{4}n_{10})n_5 + \tfrac{12859}{300}n_{10} + \tfrac{207}{40}n_{10}^2 + \tfrac{32117}{375})g_1^4\Big], \qquad (2.17a) \\
\beta_{g_2}^{(3)} =& g_2^3\Big[24(\mathrm{tr}T^2 + \mathrm{tr}B^2) + 18[(\mathrm{tr}T)^2 + (\mathrm{tr}B)^2] + 12\mathrm{tr}BT + 12\mathrm{tr}B\mathrm{tr}E + 8\mathrm{tr}E^2 \\
&+ 2(\mathrm{tr}E)^2 - (32g_3^2 + 33g_2^2)(\mathrm{tr}T + \mathrm{tr}B) - g_1^2(\tfrac{29}{5}\mathrm{tr}T + \tfrac{11}{5}\mathrm{tr}B) - \left(11g_2^2 + \tfrac{21}{5}g_1^2\right)\mathrm{tr}E \\
&- [(6n_{10} + 18)n_5 + \tfrac{118}{3}n_{10} + 18n_{10}^2 - 44]g_3^4 + [(8n_{10} + 24)g_2^2 - (\tfrac{8}{15}n_{10} + \tfrac{8}{5})g_1^2]g_3^2 \\
&- (\tfrac{13}{8}n_5^2 + (\tfrac{33}{4} + \tfrac{39}{4}n_{10})n_5 + \tfrac{99}{4}n_{10} + \tfrac{117}{8}n_{10}^2 - 35)g_2^4 + (\tfrac{1}{10}n_{10} + \tfrac{9}{5} + \tfrac{3}{10}n_5)g_1^2g_2^2 \\
&- (\tfrac{9}{40}n_5^2 + (\tfrac{3}{4}n_{10} + \tfrac{441}{100})n_5 + \tfrac{9}{40}n_{10}^2 + \tfrac{457}{25} + \tfrac{1513}{300}n_{10})g_1^4\Big], \qquad (2.17b) \\
\beta_{g_3}^{(3)} =& g_3^3\Big[18(\mathrm{tr}T)^2 + 12\mathrm{tr}T^2 + 8\mathrm{tr}BT + 18(\mathrm{tr}B)^2 + 12\mathrm{tr}B^2 + 6\mathrm{tr}E\mathrm{tr}B \\
&- (\tfrac{104}{3}g_3^2 + 12g_2^2)(\mathrm{tr}T + \mathrm{tr}B) - g_1^2(\tfrac{44}{15}\mathrm{tr}T + \tfrac{32}{15}\mathrm{tr}B) \\
&+ (\tfrac{347}{3} + \tfrac{215}{3}n_{10} - \tfrac{11}{4}n_5^2 + (\tfrac{215}{9} - \tfrac{33}{2}n_{10})n_5 - \tfrac{99}{4}n_{10}^2)g_3^4 \\
&+ [(2n_{10} + 6)g_2^2 + (\tfrac{2}{5}n_{10} + \tfrac{4}{45}n_5 + \tfrac{22}{15})g_1^2]g_3^2 \\
&- [(\tfrac{27}{4} + \tfrac{9}{4}n_{10})n_5 + \tfrac{27}{4}n_{10}^2 + \tfrac{117}{4}n_{10} + 27]g_2^4 - (\tfrac{1}{5}n_{10} + \tfrac{3}{5})g_1^2g_2^2 \\
&- (\tfrac{1}{10}n_5^2 + (\tfrac{2689}{900} + \tfrac{3}{4}n_{10})n_5 + \tfrac{27}{20}n_{10}^2 + \tfrac{1702}{75} + \tfrac{3353}{300}n_{10})g_1^4\Big]. \qquad (2.17c)
\end{aligned}$$

The three-loop results for the anomalous dimensions are as follows:

$$
\begin{aligned}
\gamma_Q^{(3)} &= k(T^3+B^3)+4BTB+4TBT+6T^2\mathrm{tr}T+B^2(6\mathrm{tr}B+2\mathrm{tr}E)\\
&+B[6\mathrm{tr}(TB)-9(\mathrm{tr}B)^2-6\mathrm{tr}B\mathrm{tr}E+18\mathrm{tr}(B^2)-(\mathrm{tr}E)^2+6\mathrm{tr}(E^2)]\\
&-9T(\mathrm{tr}T)^2+18T\mathrm{tr}(T^2)+6T\mathrm{tr}(TB)+g_1^2[T^2(\tfrac{11}{3}-k)+B^2(\tfrac{7}{15}-\tfrac{1}{5}k)]\\
&+[(3k-3)g_2^2+\tfrac{64}{3}g_3^2](T^2+B^2)+[(2-\tfrac{4}{5}k)g_1^2+18g_2^2+(8k-8)g_3^2]T\mathrm{tr}T\\
&+g_1^2B[(\tfrac{16}{5}-\tfrac{4}{5}k)\mathrm{tr}B+(\tfrac{2}{5}k-\tfrac{8}{5})\mathrm{tr}E]+g_2^2B(18\mathrm{tr}B+6\mathrm{tr}E)\\
&+8g_3^2B[(k-1)\mathrm{tr}B+\mathrm{tr}E]+g_1^4T(\tfrac{143}{900}k-\tfrac{3767}{300}-\tfrac{51}{20}n_{10}-\tfrac{17}{20}n_5)\\
&+g_1^4B(\tfrac{7}{180}k-\tfrac{633}{100}-\tfrac{27}{20}n_{10}-\tfrac{9}{20}n_5)-(\tfrac{13}{30}\mathrm{tr}T+\tfrac{7}{30}\mathrm{tr}B+\tfrac{3}{10}\mathrm{tr}E)g_1^4\\
&+(\tfrac{3}{2}k-\tfrac{59}{10})g_1^2g_2^2T+(\tfrac{3}{10}k-\tfrac{41}{10})g_1^2g_2^2B+g_1^2g_3^2T(\tfrac{64}{45}k-\tfrac{68}{5})+g_1^2g_3^2B(\tfrac{64}{45}k-\tfrac{76}{15})\\
&-g_2^4[(T+B)(\tfrac{45}{4}+\tfrac{21}{4}k+\tfrac{27}{4}n_{10}+\tfrac{9}{4}n_5)+\tfrac{45}{2}(\mathrm{tr}T+\mathrm{tr}B)+\tfrac{15}{2}\mathrm{tr}E]\\
&-4g_2^2g_3^2(T+B)+g_3^4[(T+B)(\tfrac{8}{3}-\tfrac{136}{9}k-12n_{10}-4n_5)-\tfrac{80}{3}(\mathrm{tr}T+\mathrm{tr}B)]\\
&+(\tfrac{25}{4}-\tfrac{3}{40}kn_{10}-\tfrac{9}{40}kn_5-\tfrac{27}{20}k+\tfrac{3}{10}n_{10}+\tfrac{11}{10}n_5)g_1^2g_2^4-\tfrac{8}{5}g_1^2g_2^2g_3^2\\
&+g_1^6(\tfrac{28457}{13500}-k(\tfrac{23}{600}n_{10}+\tfrac{7}{1800}n_5+\tfrac{199}{1500})+(\tfrac{1}{20}n_5+\tfrac{17}{20}+\tfrac{3}{40}n_{10})n_{10}+\tfrac{43}{180}n_5+\tfrac{1}{120}n_5^2)\\
&+g_1^4g_2^2(\tfrac{11}{100}-\tfrac{1}{200}kn_{10}-\tfrac{3}{200}kn_5-\tfrac{9}{100}k-\tfrac{1}{20}n_{10}+\tfrac{1}{20}n_5)\\
&+g_1^4g_3^2(\tfrac{194}{225}-\tfrac{2}{25}kn_{10}-\tfrac{4}{225}kn_5-\tfrac{22}{75}k+\tfrac{4}{15}n_{10}+\tfrac{2}{45}n_5)\\
&+g_1^2g_3^4(\tfrac{608}{45}-\tfrac{4}{5}kn_{10}-\tfrac{8}{45}kn_5-\tfrac{44}{15}k+\tfrac{58}{15}n_{10}+\tfrac{38}{45}n_5)\\
&+g_2^4g_3^2(50-6kn_{10}-18k+24n_{10}-2n_5)+g_2^2g_3^4(8-4kn_{10}-12k+14n_{10}-2n_5)\\
&+g_2^6(\tfrac{345}{4}+\tfrac{45}{8}kn_{10}+\tfrac{15}{8}kn_5+\tfrac{105}{4}k+\tfrac{9}{4}n_{10}n_5+\tfrac{81}{2}n_{10}+\tfrac{27}{8}n_{10}^2+\tfrac{27}{2}n_5+\tfrac{3}{8}n_5^2)\\
&+g_3^6(\tfrac{2720}{27}+k(\tfrac{40}{3}n_{10}+\tfrac{40}{9}n_5+\tfrac{160}{3})+n_{10}(4n_5+\tfrac{236}{3}+6n_{10})+\tfrac{236}{9}n_5+\tfrac{2}{3}n_5^2)
\end{aligned}
\tag{2.18}
$$

$$
\begin{aligned}
\gamma_L^{(3)} &= kE^3+E^2(6\mathrm{tr}B+2\mathrm{tr}E)\\
&+E[6\mathrm{tr}(TB)-9(\mathrm{tr}B)^2-6\mathrm{tr}B\mathrm{tr}E+18\mathrm{tr}(B^2)-(\mathrm{tr}E)^2+6\mathrm{tr}(E^2)]\\
&+g_1^2E^2(9-\tfrac{9}{5}k)+(8-2k)g_1^2E\mathrm{tr}B+(3k-3)g_2^2E^2+g_2^2E(18\mathrm{tr}B+6\mathrm{tr}E)\\
&+(8k-32)g_3^2E\mathrm{tr}B+g_1^4E(-\tfrac{549}{20}+\tfrac{27}{100}k-\tfrac{99}{20}n_{10}-\tfrac{33}{20}n_5)\\
&+g_1^4(-\tfrac{39}{10}\mathrm{tr}T-\tfrac{21}{10}\mathrm{tr}B-\tfrac{27}{10}\mathrm{tr}E)\\
&+g_1^2g_2^2E(-\tfrac{81}{10}+\tfrac{27}{10}k)+g_2^4E(-\tfrac{45}{4}-\tfrac{21}{4}k-\tfrac{27}{4}n_{10}-\tfrac{9}{4}n_5)\\
&+g_2^4(-\tfrac{45}{2}\mathrm{tr}T-\tfrac{45}{2}\mathrm{tr}B-\tfrac{15}{2}\mathrm{tr}E)+\Xi
\end{aligned}
\tag{2.19}
$$

$$
\begin{aligned}
\gamma_t^{(3)} &= (6+2k)\tilde{T}^3 + 6\tilde{T}^2\mathrm{tr}T - 2Y_t^\dagger BTY_t - 2Y_t^\dagger TBY_t + 6Y_t^\dagger B^2 Y_t \\
&+ \tilde{T}(36\mathrm{tr}(T^2) + 12\mathrm{tr}(TB) - 18(\mathrm{tr}T)^2) + Y_t^\dagger BY_t(-6\mathrm{tr}T + 12\mathrm{tr}B + 4\mathrm{tr}E) \\
&+ g_1^2\left[\tilde{T}^2(-\tfrac{1}{3}+k) + 7(1+\tfrac{k}{5})\tilde{T}\mathrm{tr}(T) + Y_t^\dagger BY_t(\tfrac{19}{15}+\tfrac{3}{5}k)\right] \\
&+ g_2^2\left[(9-3k)\tilde{T}^2 + (27-9k)\tilde{T}\mathrm{tr}T + (9-3k)Y_t^\dagger BY_t\right] \\
&+ g_3^2\left[16(k-1)\tilde{T}\mathrm{tr}T + \tfrac{64}{3}(\tilde{T}^2 + Y_t^\dagger BY_t)\right] \\
&+ g_1^4\left[\tilde{T}(-\tfrac{799}{50} - \tfrac{247}{450}k - \tfrac{18}{5}n_{10} - \tfrac{6}{5}n_5) - \tfrac{104}{15}\mathrm{tr}T - \tfrac{56}{15}\mathrm{tr}B - \tfrac{24}{5}\mathrm{tr}E\right] \\
&+ g_1^2 g_3^2\tilde{T}(-\tfrac{8}{15} - \tfrac{112}{45}k) + g_1^2 g_2^2\tilde{T}(-\tfrac{67}{5} + \tfrac{13}{5}k) \\
&+ g_2^4\tilde{T}(-\tfrac{87}{2} - \tfrac{3}{2}k - 18n_{10} - 6n_5) + g_2^2 g_3^2\tilde{T}(-88+16k) \\
&+ g_3^4\left[\tilde{T}(\tfrac{16}{3} - \tfrac{272}{9}k - 24n_{10} - 8n_5) - \tfrac{80}{3}\mathrm{tr}T - \tfrac{80}{3}\mathrm{tr}B\right] \\
&+ g_1^2 g_3^4(-\tfrac{172}{45} - \tfrac{4}{5}kn_{10} - \tfrac{8}{45}kn_5 - \tfrac{44}{15}k + \tfrac{28}{15}n_{10} + \tfrac{8}{45}n_5) \\
&+ g_1^4 g_2^2(\tfrac{36}{5} - \tfrac{2}{25}kn_{10} - \tfrac{6}{25}kn_5 - \tfrac{36}{25}k + \tfrac{2}{5}n_{10} + \tfrac{6}{5}n_5) \\
&+ g_1^4 g_3^2(\tfrac{2144}{225} - \tfrac{32}{25}kn_{10} - \tfrac{64}{225}kn_5 - \tfrac{352}{75}k + \tfrac{64}{15}n_{10} + \tfrac{32}{45}n_5) \\
&+ g_3^6(\tfrac{2720}{27} + \tfrac{40}{3}kn_{10} + \tfrac{40}{9}kn_5 + \tfrac{160}{3}k + 4n_{10}n_5 + \tfrac{236}{3}n_{10} + 6n_{10}^2 + \tfrac{236}{9}n_5 + \tfrac{2}{3}n_5^2) \\
&+ g_1^6(\tfrac{106868}{3375} - k(\tfrac{46}{75}n_{10} + \tfrac{14}{225}n_5 + \tfrac{796}{375}) + n_{10}(\tfrac{4}{5}n_5 + \tfrac{66}{5} + \tfrac{6}{5}n_{10}) + \tfrac{166}{45}n_5 + \tfrac{2}{15}n_5^2) \\
&+ g_2^2 g_3^4(60 - 4kn_{10} - 12k + 20n_{10})
\end{aligned}
\tag{2.20}
$$

$$
\begin{aligned}
\gamma_{H_1}^{(3)} &= (k+1)\left[3\mathrm{tr}(B^3) + \mathrm{tr}(E^3)\right] + 9\mathrm{tr}(T^2B) + 18\mathrm{tr}T\mathrm{tr}(TB) \\
&+ 6(\mathrm{tr}E + 3\mathrm{tr}B)\left[\mathrm{tr}(E^2) + 3\mathrm{tr}(B^2)\right] + (24-8k)g_3^2[\mathrm{tr}(TB) + 3\mathrm{tr}(B^2)] \\
&+ g_2^2[18\mathrm{tr}(TB) + (9k+9)\mathrm{tr}(B^2) + (3k+3)\mathrm{tr}(E^2)] \\
&+ g_1^2[-\tfrac{12}{5}\mathrm{tr}(TB) + \tfrac{7}{5}k\mathrm{tr}(TB) + 3\mathrm{tr}(B^2) + \tfrac{9}{5}k\mathrm{tr}(B^2) + 9\mathrm{tr}(E^2) - \tfrac{9}{5}k\mathrm{tr}(E^2)] \\
&+ g_1^4[-\tfrac{39}{10}\mathrm{tr}T - \mathrm{tr}B(\tfrac{175}{12} + \tfrac{77}{300}k + \tfrac{57}{20}n_{10} + \tfrac{19}{20}n_5) + \mathrm{tr}E(\tfrac{27}{100}k - \tfrac{603}{20} \\
&- \tfrac{99}{20}n_{10} - \tfrac{33}{20}n_5)] + g_1^2 g_2^2(-\tfrac{3}{10}\mathrm{tr}B - \tfrac{3}{2}k\mathrm{tr}B - \tfrac{81}{10}\mathrm{tr}E + \tfrac{27}{10}k\mathrm{tr}E) \\
&+ \mathrm{tr}B[g_1^2 g_3^2(-\tfrac{284}{15} + \tfrac{56}{15}k) + g_2^2 g_3^2(-132+24k)] + g_2^4[-\tfrac{45}{2}\mathrm{tr}T \\
&- \mathrm{tr}B(\tfrac{225}{4} + \tfrac{63}{4}k + \tfrac{81}{4}n_{10} + \tfrac{27}{4}n_5) - \mathrm{tr}E(\tfrac{75}{4} + \tfrac{21}{4}k + \tfrac{27}{4}n_{10} + \tfrac{9}{4}n_5)] \\
&- g_3^4\mathrm{tr}B(\tfrac{160}{3} + \tfrac{8}{3}k + 48n_{10} + 16n_5) + \Xi
\end{aligned}
\tag{2.21}
$$

$$
\begin{aligned}
\gamma_b^{(3)} &= (2k+6)\tilde{B}^3 + 6Y_b^\dagger T^2 Y_b - 2Y_b^\dagger BTY_b + Y_b^\dagger TY_b(12\mathrm{tr}T - 6\mathrm{tr}B - 2\mathrm{tr}E) \\
&- 2Y_b^\dagger TBY_b + \tilde{B}^2(6\mathrm{tr}B + 2\mathrm{tr}E) \\
&+ \tilde{B}[12\mathrm{tr}(TB) - 18(\mathrm{tr}B)^2 - 12\mathrm{tr}B\mathrm{tr}E + 36\mathrm{tr}(B^2) - 2(\mathrm{tr}E)^2 + 12\mathrm{tr}(E^2)] \\
&+ g_1^2 Y_b^\dagger TY_b(-\tfrac{29}{15} + \tfrac{3}{5}k) + g_1^2\tilde{B}^2(-\tfrac{1}{3} + \tfrac{1}{5}k) + g_1^2\tilde{B}[(7-k)\mathrm{tr}B + (k-3)\mathrm{tr}E] \\
&+ g_2^2 Y_b^\dagger TY_b(9-3k) + g_2^2\tilde{B}^2(9-3k) + g_2^2\tilde{B}[(27-9k)\mathrm{tr}B + (9-3k)\mathrm{tr}E] \\
&+ \tfrac{64}{3}g_3^2 Y_b^\dagger TY_b + \tfrac{64}{3}g_3^2\tilde{B}^2 + g_3^2\tilde{B}[(16k-16)\mathrm{tr}B + 16\mathrm{tr}E] \\
&+ g_1^4\left[\tilde{B}(-\tfrac{337}{30} - \tfrac{7}{450}k - \tfrac{12}{5}n_{10} - \tfrac{4}{5}n_5) - \tfrac{26}{15}\mathrm{tr}T - \tfrac{14}{15}\mathrm{tr}B - \tfrac{6}{5}\mathrm{tr}E\right] \\
&+ g_1^2 g_2^2\tilde{B}(-\tfrac{43}{5} + \tfrac{7}{5}k) + g_1^2 g_3^2\tilde{B}(-\tfrac{24}{5} + \tfrac{16}{9}k) + g_2^2 g_3^2\tilde{B}(-88 + 16k) \\
&+ g_2^4\tilde{B}(-\tfrac{87}{2} - \tfrac{3}{2}k - 18n_{10} - 6n_5) \\
&+ g_3^4\left[\tilde{B}(\tfrac{16}{3} - \tfrac{272}{9}k - 24n_{10} - 8n_5) - \tfrac{80}{3}\mathrm{tr}T - \tfrac{80}{3}\mathrm{tr}B\right] \\
&+ g_3^6(\tfrac{2720}{27} + \tfrac{40}{3}kn_{10} + \tfrac{40}{9}kn_5 + \tfrac{160}{3}k + 4n_{10}n_5 + \tfrac{236}{3}n_{10} + 6n_{10}^2 + \tfrac{236}{9}n_5 + \tfrac{2}{3}n_5^2) \\
&+ g_1^6(\tfrac{5629}{675} - k(\tfrac{23}{150}n_{10} + \tfrac{7}{450}n_5 + \tfrac{199}{375}) + n_{10}(\tfrac{1}{5}n_5 + \tfrac{169}{50} + \tfrac{3}{10}n_{10}) + \tfrac{427}{450}n_5 + \tfrac{1}{30}n_5^2) \\
&+ g_1^4 g_2^2(\tfrac{9}{5} - \tfrac{1}{50}kn_{10} - \tfrac{3}{50}kn_5 - \tfrac{9}{25}k + \tfrac{1}{10}n_{10} + \tfrac{3}{10}n_5) \\
&+ g_1^4 g_3^2(\tfrac{728}{225} - \tfrac{8}{25}kn_{10} - \tfrac{16}{225}kn_5 - \tfrac{88}{75}k + \tfrac{16}{15}n_{10} + \tfrac{8}{45}n_5) \\
&+ g_1^2 g_3^4(\tfrac{452}{45} - \tfrac{4}{5}kn_{10} - \tfrac{8}{45}kn_5 - \tfrac{44}{15}k + \tfrac{52}{15}n_{10} + \tfrac{32}{45}n_5) \\
&+ g_2^2 g_3^4(60 - 4kn_{10} - 12k + 20n_{10})
\end{aligned}
\tag{2.22}
$$

$$
\begin{aligned}
\gamma_{H_2}^{(3)} &= 54\mathrm{tr}T\mathrm{tr}(T^2) + 3(k+1)\mathrm{tr}(T^3) + 18\mathrm{tr}B\mathrm{tr}(TB) + 9\mathrm{tr}(BTB) + 6\mathrm{tr}E\mathrm{tr}(TB) \\
&+ g_1^2((\tfrac{57}{5} - \tfrac{3}{5}k)\mathrm{tr}(T^2) + (\tfrac{6}{5} + \tfrac{1}{5}k)\mathrm{tr}(TB)) + g_2^2[(9+9k)\mathrm{tr}(T^2) + 18\mathrm{tr}(TB)] \\
&+ g_3^2[(72-24k)\mathrm{tr}(T^2) + (24-8k)\mathrm{tr}(TB)] \\
&- g_1^4\left[(\tfrac{2123}{60} + \tfrac{13}{60}k + \tfrac{43}{20}n_5 + \tfrac{129}{20}n_{10})\mathrm{tr}T + \tfrac{21}{10}\mathrm{tr}B + \tfrac{27}{10}\mathrm{tr}E\right] \\
&+ [g_1^2 g_2^2(\tfrac{21}{10}k - \tfrac{57}{10}) + g_1^2 g_3^2(\tfrac{104}{15}k - \tfrac{124}{3}) + g_2^2 g_3^2(24k - 132)]\mathrm{tr}T \\
&+ g_2^4(\mathrm{tr}T(-\tfrac{225}{4} - \tfrac{63}{4}k - \tfrac{81}{4}n_{10} - \tfrac{27}{4}n_5) - \tfrac{45}{2}\mathrm{tr}B - \tfrac{15}{2}\mathrm{tr}E) \\
&- g_3^4(\tfrac{160}{3}\mathrm{tr}T + \tfrac{8}{3}k\mathrm{tr}T + 48n_{10}\mathrm{tr}T + 16n_5\mathrm{tr}T) + \Xi
\end{aligned}
\tag{2.23}
$$

$$
\begin{aligned}
\gamma_\tau^{(3)} &= (6+2k)\tilde{E}^3 + (6\mathrm{tr}B + 2\mathrm{tr}E)\tilde{E}^2 \\
&+ \tilde{E}(12\mathrm{tr}(TB) - 18(\mathrm{tr}B)^2 - 12\mathrm{tr}B\mathrm{tr}E + 36\mathrm{tr}(B^2) - 2(\mathrm{tr}E)^2 + 12\mathrm{tr}(E^2)) \\
&+ g_1^2\tilde{E}^2(\tfrac{9}{5} + \tfrac{9}{5}k) + g_2^2\tilde{E}^2(9-3k) + g_1^2\tilde{E}((\tfrac{107}{5} + \tfrac{7}{5}k)\mathrm{tr}B + (\tfrac{9}{5} + \tfrac{9}{5}k)\mathrm{tr}E) \\
&+ g_3^2\tilde{E}\mathrm{tr}B(16k-64) + g_2^2\tilde{E}(\mathrm{tr}B(27-9k) + \mathrm{tr}E(9-3k)) \\
&+ g_1^4\tilde{E}(-\tfrac{1503}{50} - \tfrac{27}{10}k - \tfrac{36}{5}n_{10} - \tfrac{12}{5}n_5) + g_1^2g_2^2\tilde{E}(-27 + \tfrac{27}{5}k) \\
&+ g_1^4(-\tfrac{78}{5}\mathrm{tr}T - \tfrac{42}{5}\mathrm{tr}B - \tfrac{54}{5}\mathrm{tr}E) + g_2^4\tilde{E}(-\tfrac{87}{2} - \tfrac{3}{2}k - 18n_{10} - 6n_5) \\
&+ g_1^6(\tfrac{7899}{125} - \tfrac{69}{50}kn_{10} - \tfrac{7}{50}kn_5 - \tfrac{597}{125}k + \tfrac{9}{5}n_{10}n_5 + \tfrac{57}{2}n_{10} + \tfrac{27}{10}n_{10}^2 + \tfrac{79}{10}n_5 + \tfrac{3}{10}n_5^2) \\
&+ g_1^4g_2^2(\tfrac{81}{5} - \tfrac{9}{50}kn_{10} - \tfrac{27}{50}kn_5 - \tfrac{81}{25}k + \tfrac{9}{10}n_{10} + \tfrac{27}{10}n_5) \\
&+ g_1^4g_3^2(\tfrac{264}{5} - \tfrac{72}{25}kn_{10} - \tfrac{16}{25}kn_5 - \tfrac{264}{25}k + \tfrac{72}{5}n_{10} + \tfrac{16}{5}n_5)
\end{aligned}
\tag{2.24}
$$

where $k = 6\zeta(3)$, and

$$
\begin{aligned}
\Xi &= g_2^6(\tfrac{345}{4} + k(\tfrac{45}{8}n_{10} + \tfrac{15}{8}n_5 + \tfrac{105}{4}) + n_{10}(\tfrac{9}{4}n_5 + \tfrac{81}{2} + \tfrac{27}{8}n_{10}) + \tfrac{27}{2}n_5 + \tfrac{3}{8}n_5^2) \\
&+ g_1^6(\tfrac{1839}{100} - k(\tfrac{69}{200}n_{10} + \tfrac{7}{200}n_5 + \tfrac{597}{500}) + n_{10}(\tfrac{9}{20}n_5 + \tfrac{753}{100} + \tfrac{27}{40}n_{10}) + \tfrac{211}{100}n_5 + \tfrac{3}{40}n_5^2) \\
&+ g_1^4g_2^2(\tfrac{27}{100} - \tfrac{9}{200}kn_{10} - \tfrac{27}{200}kn_5 - \tfrac{81}{100}k - \tfrac{9}{20}n_{10} + \tfrac{9}{20}n_5) \\
&+ g_1^4g_3^2(\tfrac{66}{5} - \tfrac{18}{25}kn_{10} - \tfrac{4}{25}kn_5 - \tfrac{66}{25}k + \tfrac{18}{5}n_{10} + \tfrac{4}{5}n_5) \\
&+ g_1^2g_2^4(\tfrac{9}{4} - \tfrac{3}{40}kn_{10} - \tfrac{9}{40}kn_5 - \tfrac{27}{20}k - \tfrac{3}{10}n_{10} + \tfrac{9}{10}n_5) \\
&+ g_2^4g_3^2(90 - 6kn_{10} - 18k + 30n_{10}).
\end{aligned}
\tag{2.25}
$$

In terms of the anomalous dimensions, the Yukawa β-functions are:

$$
\beta_{Y_t} = \gamma_Q Y_t + Y_t(\gamma_t + \gamma_{H_2}), \quad \beta_{Y_b} = \gamma_Q Y_b + Y_b(\gamma_b + \gamma_{H_1}), \quad \beta_{Y_\tau} = \gamma_L Y_\tau + Y_\tau(\gamma_\tau + \gamma_{H_1}),
\tag{2.26}
$$

and the β-function for the Higgs μ-term is

$$
\beta_\mu = \mu(\gamma_{H_2} + \gamma_{H_1}).
\tag{2.27}
$$

We will also require the anomalous dimensions of the constituents of the extra 5 and 10 representations, which are easily obtained by setting $T = B = E = 0$, except retaining terms that contain T, B, E *only* inside traces; such terms occur for the first time at three loops.

From the above expressions for β_{g_i} and γ we have calculated the three-loop soft β-functions using Eq. (2.3) and FORM. The resulting expressions are very unwieldy; as an example we give the one, two and three-loop results for $\beta_{m^2_{Q_t}}$, in the approximation that we retain only g_3^2 and the top quark Yukawa coupling λ_t (in what follows we denote the third generation squarks as Q_t, t^c, b^c, and the first or second generation squarks as Q_u, u^c, d^c):

$$\beta^{(1)}_{m^2_{Q_t}} = 2\lambda_t^2(\Sigma_t + A_t^2) - 8(\tfrac{1}{60}g_1^2M_1^2 + \tfrac{3}{4}g_2^2M_2^2 + \tfrac{4}{3}g_3^2M_3^2) \tag{2.28a}$$

$$\begin{aligned}\beta^{(2)}_{m^2_{Q_t}} &= -20\lambda_t^4(\Sigma_t + 2A_t^2) + 16g_3^4M_3^2(n_5 + 3n_{10} - \tfrac{8}{3}) \\ &+ \tfrac{16}{3}g_3^4(2m^2_{Q_t} + m^2_{t^c} + m^2_{b^c} + (n_{10}+2)(m^2_{u^c} + 2m^2_{Q_u}) + (n_5+2)m^2_{d^c})\end{aligned} \tag{2.28b}$$

$$\begin{aligned}\beta^{(3)}_{m^2_{Q_t}} &= [(1280k + \tfrac{20512}{9} + 16n_5^2 + (\tfrac{6224}{9} + \tfrac{320}{3}k)(n_5+3n_{10}) \\ &+ 96n_{10}n_5 + 144n_{10}^2)M_3^2 + (\tfrac{320}{9} - \tfrac{16}{3}(n_5+3n_{10}))(m^2_{t^c} + m^2_{b^c} + 2m^2_{Q_t}) \\ &+ (2m^2_{Q_u} + m^2_{u^c})(\tfrac{640}{9} - \tfrac{32}{3}n_5 + \tfrac{32}{9}n_{10} - \tfrac{16}{3}n_5n_{10} - 16n_{10}^2) \\ &+ m^2_{d^c}(\tfrac{640}{9} + \tfrac{224}{9}n_5 - 32n_{10} - 16n_5n_{10} - \tfrac{16}{3}n_5^2)]g_3^6 \\ &- [(288 + \tfrac{544}{3}k + 48(n_5+3n_{10}))M_3^2 - (192 + \tfrac{1088}{9}k + 32(n_5+3n_{10}))A_tM_3 \\ &+ (\tfrac{272}{9}k + \tfrac{176}{3} + 8(n_5+3n_{10}))(\Sigma_t + A_t^2)]\lambda_t^2g_3^4 \\ &+ (\tfrac{160}{3} + 32k)\left[M_3^2 - 2A_tM_3 + \Sigma_t + 2A_t^2\right]\lambda_t^4g_3^2 \\ &+ (6k+90)(\Sigma_t + 3A_t^2)\lambda_t^6,\end{aligned} \tag{2.28c}$$

where $\Sigma_t = m^2_{Q_t} + m_2^2 + m^2_{t^c}$. For this special case, and also with $n_5 = n_{10} = 0$, the three-loop result, Eq. (2.28*c*), was given in Ref. [22], except that in the corresponding expressions in this reference the squark masses of different generations are not clearly distinguished (as they must be since the third generation evolves differently from the other two). Complete results for the three-loop β-functions including all three gauge couplings and $n_g \times n_g$ Yukawa matrices are available at Ref. [7].

In our analysis we do include "tadpole" contributions, corresponding to renormalisation of the Fayet-Iliopoulos (FI) D-term at one and two loops. These contributions are not expressible exactly in terms of β_{g_i}, γ; for a discussion, and three-loop results for the MSSM, see Ref. [23]. For universal boundary conditions, the FI term is very small at low energies if it is zero at gauge unification; including the three-loop (FI) effects would have a negligible effect on our results.

3. The Snowmass Benchmark Points

In this section we examine the effect of the three-loop corrections on the standard running analysis, that is for $n_5 = n_{10} = 0$. We will focus on the standard treatment with universal boundary conditions at gauge unification, often termed CMSSM or MSUGRA. Thus we assume that at M_X we have universal soft scalar masses (m_0), gaugino masses[3] ($m_{\frac{1}{2}}$) and A-parameters (A), and work in the third-generation-only Yukawa coupling approximation. This is for ease of comparison with existing results rather than because we find the scenario particularly compelling. We will present results for the set of MSUGRA Snowmass Benchmark Points shown in Table 1:

Point	$\tan\beta$	$m_{\frac{1}{2}}$	m_0	A	signμ
SPS1a	10	250GeV	100GeV	-100GeV	$+$
SPS1b	30	400GeV	200GeV	0	$+$
SPS2	10	300GeV	1450GeV	0	$+$
SPS3	10	400GeV	90GeV	0	$+$
SPS4	50	300GeV	400GeV	0	$+$
SPS5	5	300GeV	150GeV	-1TeV	$+$
SPS6	10	see footnote[3]	150GeV	0	$+$

Table 1: Input parameters for the SPS Benchmark Points

Other input parameters are shown in Table 2:

$m_t^{\rm pole}$	$m_b^{\rm pole}$	$m_\tau^{\rm pole}$	$\alpha_3(M_Z)$	$\alpha_2(M_Z)$	$\alpha_1(M_Z)$
178GeV	4.9GeV	1.777GeV	0.1172	0.033823	0.016943

Table 2: Input parameters for the running analysis

In Table 2 the input couplings $\alpha_{1\ldots3}$ correspond to the Standard Model $\overline{\rm MS}$ results; we calculate the appropriate dimensionless coupling input values for the running analysis by an iterative procedure involving the sparticle spectrum. We define gauge unification

[3] except for the SPS6 point. The SPS6 point corresponds to non-unified gaugino masses, $M_1 = 480$GeV, $M_2 = M_3 = 300$GeV.

to be the scale where α_2 and α_1 meet; we speed up the determination of this by (at each iteration) adjusting the unification scale using the solution of the one-loop β-functions for the gauge couplings from the previous value of the scale. We employ one-loop radiative corrections as detailed in Ref. [24] [4]; thus we run up from M_Z using the full supersymmetric β-functions. For most particles we evaluate the pole mass at a renormalisation scale equal to the pole mass itself, and determine this value by iteration; the exception being the light CP-even Higgs, where we use a scale equal to the average squark mass.

3.1. Benchmark point SPS 1a

This point is a "typical" point in MSUGRA parameter space. In Table 3 we compare our results for a selection of sparticle masses (at $n_5 = n_{10} = 0$) with the spread of results taken from Ref. [9], denoted AKP (note our convention that the predominantly right-handed top squark is $\tilde{t}_2$).

[4] In the first line of Eq. 37 of Ref. [24], the first term in the square bracket should read $-(m^2_{\tilde{t}_1} + m^2_{\tilde{t}_2})B_0(m_{\tilde{t}_2}, m_{\tilde{t}_1}, 0)$: i.e. it should have a minus sign. The corresponding exact result in Eq. D49 is correct, however.

mass	1loop	2loops	3loops	AKP
$\tilde{g}$	628	613	611	$604 - 612$
$\tilde{t}_1$	594	590	583	$577 - 588$
$\tilde{t}_2$	400	399	391	$396 - 401$
$\tilde{u}_L$	573	565	557	$565 - 569$
$\tilde{u}_R$	552	548	539	$547 - 549$
$\tilde{b}_1$	520	514	507	$514 - 518$
$\tilde{b}_2$	551	548	540	$539 - 548$
$\tilde{d}_L$	579	571	563	$571 - 574$
$\tilde{d}_R$	551	548	539	$546 - 548$
$\tilde{\tau}_1$	212	207	206	$208 - 211$
$\tilde{\tau}_2$	139	135	135	$134 - 136$
$\tilde{e}_L$	209	202	202	$204 - 207$
$\tilde{e}_R$	147	144	144	$143 - 146$
$\tilde{\nu}_e$	192	186	185	$186 - 191$
$\tilde{\nu}_\tau$	191	185	184	$185 - 191$
χ_1	104	97	97	$95.6 - 97.4$
χ_2	193	180	179	$181 - 182$
χ_3	351	369	364	$362 - 371$
χ_4	376	388	384	$381 - 390$
$\chi_1^\pm$	193	179	178	$180 - 182$
$\chi_2^\pm$	376	388	384	$380 - 390$
h	114	114	114	$112 - 115$
H	392	403	399	$403 - 407$
A	391	403	399	$400 - 406$
$H^\pm$	400	412	408	$410 - 415$

Table 3: Sparticle masses (in GeV) for the SPS1a point

We would expect our two-loop results to correspond most closely to AKP and we see that they are indeed broadly consistent, typically being within the range defined by the other programs or within a GeV of it. The effect of inclusion of three-loop running is never greater than 2%; note, however, that the shift caused by three-loop running effects is comparable for $\tilde{u}_L$ and larger for $\tilde{t}_2, \tilde{u}_R$ than that produced by two-loop running effects.

3.2. Benchmark point SPS 1b

This is another "typical" point but with a higher value of $\tan\beta$. Our results are given in Table 4.

mass	1loop	2loops	3loops	AKP
$\tilde{g}$	967	946	943	$933 - 943$
$\tilde{t}_1$	848	841	832	$836 - 839$
$\tilde{t}_2$	657	656	646	$652 - 661$
$\tilde{u}_L$	891	878	868	$878 - 882$
$\tilde{u}_R$	854	849	837	$848 - 850$
$\tilde{b}_1$	781	773	763	$773 - 778$
$\tilde{b}_2$	831	827	816	$819 - 828$
$\tilde{d}_L$	895	882	872	$882 - 885$
$\tilde{d}_R$	851	847	835	$844 - 848$
$\tilde{\tau}_1$	353	347	346	$347 - 349$
$\tilde{\tau}_2$	208	199	200	$196 - 202$
$\tilde{e}_L$	348	339	338	$341 - 342$
$\tilde{e}_R$	258	254	254	$253 - 256$
$\tilde{\nu}_e$	338	329	328	$329 - 332$
$\tilde{\nu}_\tau$	328	318	318	$319 - 322$
χ_1	173	162	162	$159 - 163$
χ_2	327	305	304	$308 - 308$
χ_3	507	532	526	$521 - 534$
χ_4	526	546	541	$534 - 546$
$\chi_1^\pm$	327	305	304	$307 - 308$
$\chi_2^\pm$	526	547	541	$535 - 547$
h	118	118	118	$117 - 119$
H	528	544	539	$540 - 544$
A	529	545	540	$538 - 544$
$H^\pm$	535	551	547	$547 - 551$

Table 4: Sparticle masses (in GeV) for the SPS1b point

3.3. Benchmark point SPS 2

This is a "focus point region" point [25], characterised by the large value of m_0. Our results are given in Table 5.

mass	1loop	2loops	3loops	AKP
$\tilde{g}$	835	816	814	$778 - 805$
$\tilde{t}_1$	1322	1292	1287	$1291 - 1318$
$\tilde{t}_2$	942	921	913	$913 - 942$
$\tilde{u}_L$	1597	1562	1558	$1566 - 1591$
$\tilde{u}_R$	1584	1556	1552	$1556 - 1581$
$\tilde{b}_1$	1303	1273	1268	$1280 - 1309$
$\tilde{b}_2$	1571	1544	1540	$1527 - 1568$
$\tilde{d}_L$	1600	1564	1560	$1567 - 1593$
$\tilde{d}_R$	1584	1556	1553	$1555 - 1580$
$\tilde{\tau}_1$	1463	1454	1454	$1455 - 1460$
$\tilde{\tau}_2$	1444	1440	1441	$1439 - 1443$
$\tilde{e}_L$	1468	1459	1459	$1460 - 1465$
$\tilde{e}_R$	1457	1453	1453	$1453 - 1455$
$\tilde{\nu}_e$	1465	1456	1456	$1457 - 1463$
$\tilde{\nu}_\tau$	1459	1450	1450	$1451 - 1457$
χ_1	132	123	123	$121 - 124$
χ_2	257	237	237	$240 - 241$
χ_3	562	579	582	$528 - 596$
χ_4	574	589	592	$539 - 605$
$\chi_1^\pm$	257	237	237	$240 - 241$
$\chi_2^\pm$	574	590	592	$539 - 605$
h	119	119	119	$117 - 117$
H	1548	1545	1546	$1542 - 1555$
A	1548	1545	1546	$1532 - 1555$
$H^\pm$	1550	1547	1548	$1544 - 1557$

Table 5: Sparticle masses (in GeV) for the SPS2 point

3.4. Benchmark point SPS 3

This is a "co-annihilation region" point, its distinctive feature being a light stau not much heavier than the neutralino LSP. Our results are given in Table 6.

mass	1loop	2loops	3loops	AKP
$\tilde{g}$	964	943	940	$930 - 940$
$\tilde{t}_1$	851	845	835	$836 - 843$
$\tilde{t}_2$	645	644	634	$640 - 650$
$\tilde{u}_L$	872	860	849	$861 - 863$
$\tilde{u}_R$	835	830	818	$828 - 831$
$\tilde{b}_1$	794	787	776	$786 - 793$
$\tilde{b}_2$	830	826	814	$816 - 825$
$\tilde{d}_L$	876	864	853	$864 - 867$
$\tilde{d}_R$	831	828	816	$825 - 829$
$\tilde{\tau}_1$	300	291	290	$293 - 294$
$\tilde{\tau}_2$	180	173	173	$172 - 176$
$\tilde{e}_L$	299	288	288	$291 - 293$
$\tilde{e}_R$	186	181	181	$179 - 183$
$\tilde{\nu}_e$	287	277	276	$277 - 281$
$\tilde{\nu}_\tau$	286	276	275	$276 - 280$
χ_1	172	161	161	$158 - 162$
χ_2	325	302	301	$305 - 306$
χ_3	512	538	531	$528 - 540$
χ_4	533	554	548	$543 - 555$
$\chi_1^\pm$	324	302	301	$304 - 306$
$\chi_2^\pm$	533	554	548	$542 - 555$
h	117	118	117	$116 - 118$
H	579	597	591	$593 - 600$
A	579	597	591	$589 - 600$
$H^\pm$	585	603	597	$598 - 605$

Table 6: Sparticle masses (in GeV) for the SPS3 point

3.5. Benchmark point SPS4

This is a point with large $\tan\beta$. Our results are given in Table 7.

mass	1loop	2loops	3loops	AKP
$\tilde{g}$	759	743	741	$729-738$
$\tilde{t}_1$	705	700	693	$693-697$
$\tilde{t}_2$	544	541	533	$540-544$
$\tilde{u}_L$	777	764	757	$766-772$
$\tilde{u}_R$	755	747	739	$747-751$
$\tilde{b}_1$	624	619	611	$614-619$
$\tilde{b}_2$	693	690	683	$679-692$
$\tilde{d}_L$	782	769	761	$770-776$
$\tilde{d}_R$	753	746	738	$746-749$
$\tilde{\tau}_1$	423	420	420	$414-421$
$\tilde{\tau}_2$	272	268	268	$253-269$
$\tilde{e}_L$	455	450	449	$451-452$
$\tilde{e}_R$	419	417	418	$417-419$
$\tilde{\nu}_e$	447	441	441	$442-445$
$\tilde{\nu}_\tau$	395	390	390	$387-393$
χ_1	128	120	120	$119-121$
χ_2	242	226	225	$228-228$
χ_3	400	419	415	$406-420$
χ_4	420	435	431	$422-436$
$\chi_1^\pm$	242	226	225	$227-228$
$\chi_2^\pm$	421	436	432	$422-436$
h	116	116	116	$114-116$
H	370	386	385	$355-367$
A	371	388	387	$355-367$
$H^\pm$	381	397	396	$366-379$

Table 7: Sparticle masses (in GeV) for the SPS4 point

3.6. Benchmark point SPS 5

mass	1loop	2loops	3loops	AKP
$\tilde{g}$	743	729	727	$719 - 729$
$\tilde{t}_1$	653	654	646	$629 - 651$
$\tilde{t}_2$	265	278	263	$258 - 280$
$\tilde{u}_L$	684	677	668	$676 - 685$
$\tilde{u}_R$	658	656	646	$655 - 660$
$\tilde{b}_1$	563	563	554	$554 - 567$
$\tilde{b}_2$	654	653	643	$630 - 656$
$\tilde{d}_L$	688	681	673	$681 - 689$
$\tilde{d}_R$	656	655	645	$653 - 658$
$\tilde{\tau}_1$	264	259	258	$259 - 262$
$\tilde{\tau}_2$	186	182	183	$182 - 184$
$\tilde{e}_L$	263	257	257	$258 - 261$
$\tilde{e}_R$	195	192	193	$192 - 194$
$\tilde{\nu}_e$	251	245	245	$246 - 249$
$\tilde{\nu}_\tau$	249	243	243	$244 - 247$
χ_1	128	120	120	$119 - 120$
χ_2	247	229	228	$230 - 236$
χ_3	608	626	621	$626 - 631$
χ_4	621	637	632	$637 - 641$
$\chi_1^\pm$	247	229	228	$230 - 236$
$\chi_2^\pm$	620	637	632	$636 - 641$
h	117	118	118	$116 - 122$
H	667	682	676	$681 - 694$
A	667	682	677	$682 - 690$
$H^\pm$	672	687	681	$687 - 698$

Table 8: Sparticle masses (in GeV) for the SPS5 point with $m_t = 178$GeV

This point differs from the previous ones in having a large value of the A-parameter. The contributions of μ, A to the off-diagonal term in the stop mass matrix have the same sign, and the magnitude of A is large, resulting in a light stop. For this point we have

calculated both using in Table 8 $m_t = 178$GeV (as for the previous tables) and for comparison in Table 9 with $m_t = 174.3$GeV. This illustrates the sensitivity to the input m_t, with the light stop changing over 20GeV due to this small change in m_t.

mass	1loop	2loops	3loops	AKP
$\tilde{g}$	743	729	727	$718 - 728$
$\tilde{t}_1$	652	653	645	$628 - 649$
$\tilde{t}_2$	243	257	240	$232 - 258$
$\tilde{u}_L$	684	677	668	$676 - 684$
$\tilde{u}_R$	658	656	646	$653 - 660$
$\tilde{b}_1$	561	560	551	$551 - 564$
$\tilde{b}_2$	654	653	643	$629 - 655$
$\tilde{d}_L$	689	681	673	$680 - 689$
$\tilde{d}_R$	656	655	645	$651 - 658$
$\tilde{\tau}_1$	264	259	258	$258 - 262$
$\tilde{\tau}_2$	186	182	182	$182 - 184$
$\tilde{e}_L$	263	257	257	$258 - 260$
$\tilde{e}_R$	195	192	192	$192 - 194$
$\tilde{\nu}_e$	251	245	245	$246 - 249$
$\tilde{\nu}_\tau$	249	243	243	$244 - 246$
χ_1	128	120	120	$119 - 121$
χ_2	247	229	228	$230 - 236$
χ_3	615	632	628	$632 - 637$
χ_4	628	644	639	$643 - 646$
$\chi_1^\pm$	247	229	228	$230 - 236$
$\chi_2^\pm$	627	643	639	$643 - 646$
h	115	115	115	$112 - 119$
H	674	688	683	$687 - 693$
A	674	688	683	$689 - 693$
$H^\pm$	679	692	687	$694 - 702$

Table 9: Sparticle masses (in GeV) for the SPS5 point with $m_t = 174.3$GeV

3.7. Benchmark point SPS6

This is a point with un-unified gaugino masses so we are unable to compare with Ref. [9]. We instead use the paper by Ghodbane and Martyn (GM), Ref. [11], which also compares the results for various programs (Isajet, Susygen and Pythia). The results for these three programs are reasonably consistent with each other; this is due to some extent, however, to the fact that the Isajet gauge unification outputs are used as inputs for the other two programs; in our table we show only the Isajet predictions. Agreement with our results is less impressive; however we should notice that Ref. [11] uses an earlier version of Isajet (7.58) than Ref. [9]. Thus if we return to SPS1a and compare the Isajet 7.58 prediction for the gluino mass (595GeV) with the Isajet 7.69 one of 612GeV obtained from Ref. [9], we can anticipate that for SPS6 the more recent Isajet would give results more consistent with our (two-loop) ones, making the reasonable assumption that the newer version will give, for example, a higher gluino mass prediction for SPS6 as well. Our results for SPS6 are given in Table 10.

mass	1loop	2loops	3loops	GM
$\tilde{g}$	744	726	724	708
$\tilde{t}_1$	686	681	673	661
$\tilde{t}_2$	498	496	488	476
$\tilde{u}_L$	684	674	665	639
$\tilde{u}_R$	665	659	650	628
$\tilde{b}_1$	620	613	605	589
$\tilde{b}_2$	657	652	643	624
$\tilde{d}_L$	689	679	670	644
$\tilde{d}_R$	658	653	644	622
$\tilde{\tau}_1$	278	271	271	270
$\tilde{\tau}_2$	235	229	229	228
$\tilde{e}_L$	274	266	266	265
$\tilde{e}_R$	243	238	238	237
$\tilde{\nu}_e$	261	253	253	252
$\tilde{\nu}_\tau$	260	252	252	252
χ_1	201	190	190	189
χ_2	239	222	221	218
χ_3	399	419	414	399
χ_4	425	439	435	420
$\chi_1^\pm$	237	220	219	215
$\chi_2^\pm$	423	438	434	419
h	115	115	115	115
H	469	481	477	464
A	469	481	477	463
$H^\pm$	477	489	484	470

Table 10: Sparticle masses (in GeV) for the SPS6 point

3.8. Discussion

A clear feature of the results is that the corrections due to two and three-loop running can be quite large for squarks, but are typically smaller for weakly-interacting particles. In particular the light CP-even Higgs mass is very stable. The large three-loop α_3 corrections stem mainly from the M_3^2 contributions to the three-loop m^2 β-functions; note that for

the only MSUGRA point such that $m_0 > m_{\frac{1}{2}}$, i.e. SPS2, the three-loop correction to the squark masses is *smaller* than the two-loop one.

Generally speaking we would anticipate that for regions of parameter space where the three-loop corrections are comparable to or exceed the two-loop ones, the four-loop ones will be at least as large. This suggests that we are already at three loops approaching the asymptotic region for the β-functions. So it appears that squark mass predictions with an accuracy greater than a few per cent will not be possible using perturbation theory.

Overall our results agree reasonably well with those of existing programs [9]. One place where we have a significant difference is for the $H, A, H^{\pm}$ results for SPS4. This is a large $\tan\beta$ point; however our results for the b-squark and d-squark masses (which one would expect to be sensitive to large $\tan\beta$) agree quite well, so for the moment we have no explanation for this discrepancy.

4. The Semi-perturbative Region

The addition of additional matter representations in complete SU_5 multiplets does not affect gauge unification (and the unification scale) at one loop. Beyond one loop this is no longer the case, and increasing the amount of matter relevant to the running analysis requires the presumption of larger threshold corrections at the unification scale in order to restore gauge unification; one is thus forced to argue that the success of gauge unification in the MSSM is coincidental [5].

[5] Historically gauge unification was implemented by using $\alpha_3(M_Z)$ as an input and computing $\sin^2\theta_W$, although the latter was more accurately measured, because $\sin^2\theta_W$ varies very slowly with $\alpha_3(M_Z)$, and conversely (of course) $\alpha_3(M_Z)$ varies rapidly as a function of $\sin^2\theta_W$. The current experimental results for $\alpha_3(M_Z)$ already require us to suppose the existence of *some* high scale radiative corrections in the MSSM; but the fact remains that things get worse as we add more matter[13].

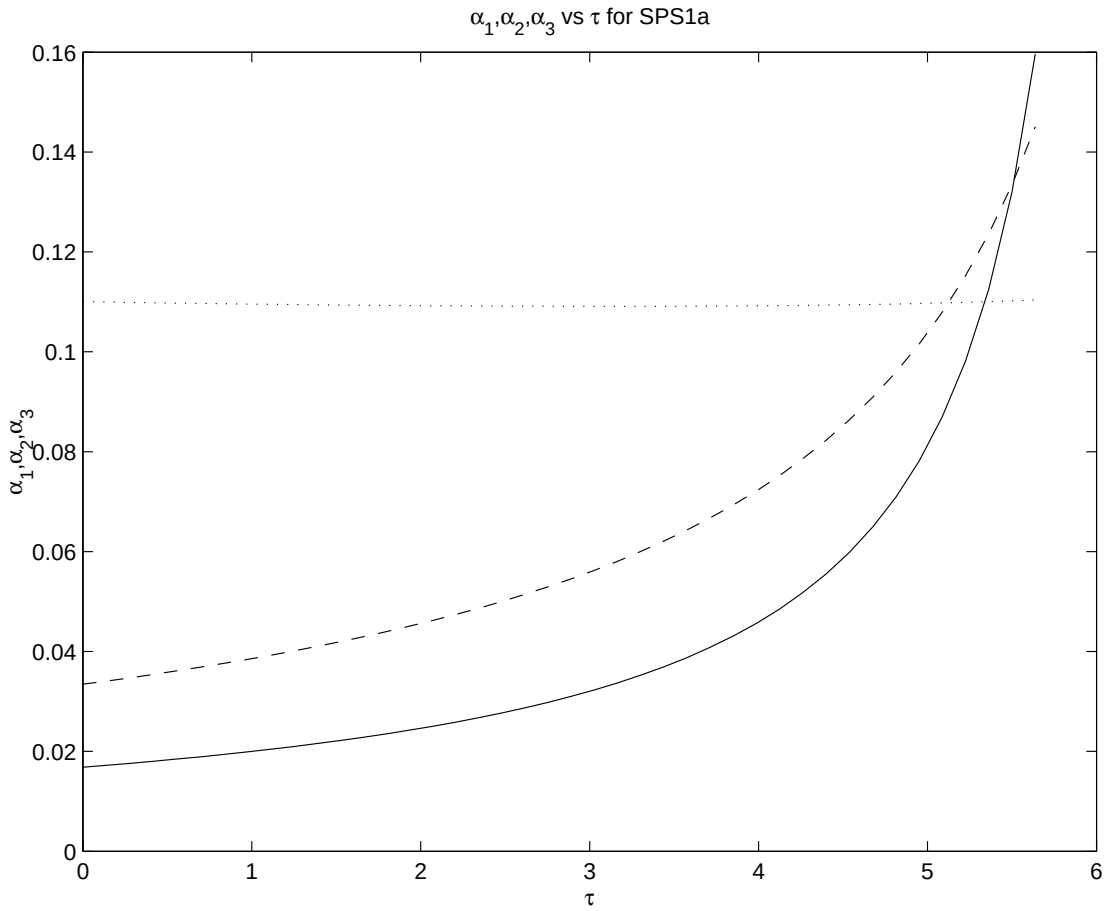

Fig.1: Gauge coupling unification for $n_{10} = 1.7$. Solid, dashed, and dotted lines correspond to $\alpha_1, \alpha_2, \alpha_3$ respectively.

In Fig. 1 we show the evolution of the gauge couplings $\alpha_i = g_i^2/(4\pi)$ for $n_{10} = 1.7$, using three-loop β-functions for all couplings. (As remarked in Ref. [12], the mass scale of these additional multiplets being unknown it makes sense to parametrise their effects by taking n_5, n_{10} to be continuous variables.) The couplings are plotted against $\tau = \frac{1}{2\pi}\ln(Q/M_Z)$; evidently we are still in the perturbative regime. The input parameters at M_Z correspond to a typical supersymmetric mass spectrum; specifically, the Benchmark point SPS1a. One sees clearly the need for large corrections to restore gauge unification.

We gave a number of examples of the effect of additional matter on the sparticle spectrum predictions in a previous paper[15]; here we contrast the effect on the first and third generation squark masses. Thus in Fig 2 we plot, for the SPS5 point, the ratio of the $\tilde{u}_L$ and gluino masses against n_{10} for $n_5 = 0$; as already noted in Ref. [12], the mass increases with n_{10}. It is interesting that the effect of the three-loop correction to this ratio almost precisely cancels the two-loop correction, for all n_{10}. We contrast this with Fig 3

where we show the behaviour of the light stop mass for the same SPS point; in this case the ratio decreases smoothly, and the three-loop correction only cancels the two-loop one at $n_{10} = 0$. For the SPS5 point the electroweak vacuum fails around $n_{10} = 0.48$. (The change in this value and in Fig. 3 from our previous paper[15] is due to the change in the input top pole mass, and to an improved treatment of the Higgs potential minimisation.)

In Fig. 4 we plot the light CP-even Higgs mass for SPS1a as a function of n_{10} (for $n_5 = 0$). We see that it is fairly stable both with respect to loop corrections and the addition of extra matter. In the case of SPS1a the electroweak vacuum fails at around $n_{10} = 1.8$.

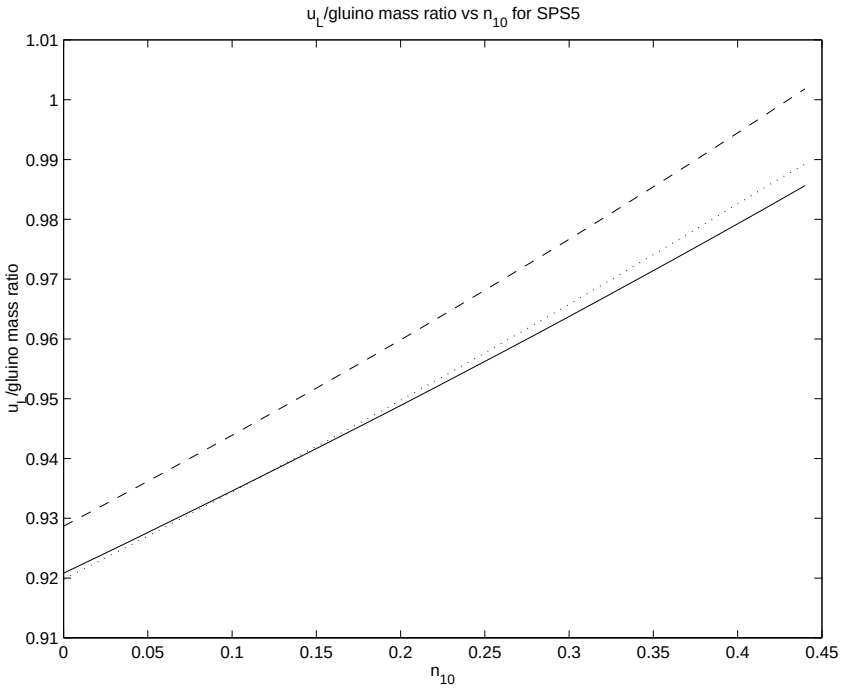

Fig.2: Plot of the $\tilde{u}_L$/gluino mass ratio against n_{10} for SPS5. Solid, dashed and dotted lines correspond to one, two and three-loop running respectively.

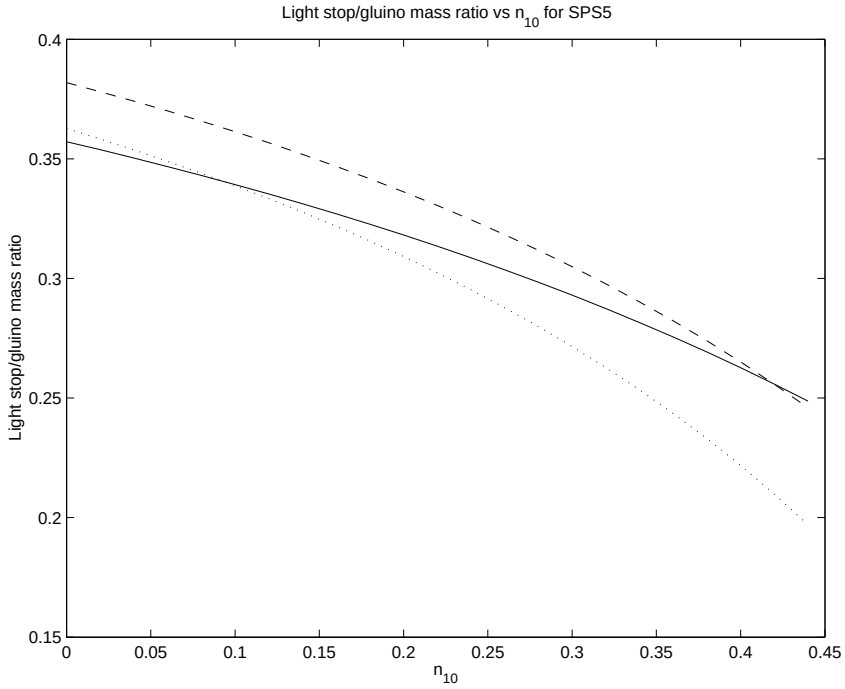

Fig.3: Plot of the light stop/gluino mass ratio against n_{10} for SPS5. Solid, dashed and dotted lines correspond to one, two and three-loop running respectively.

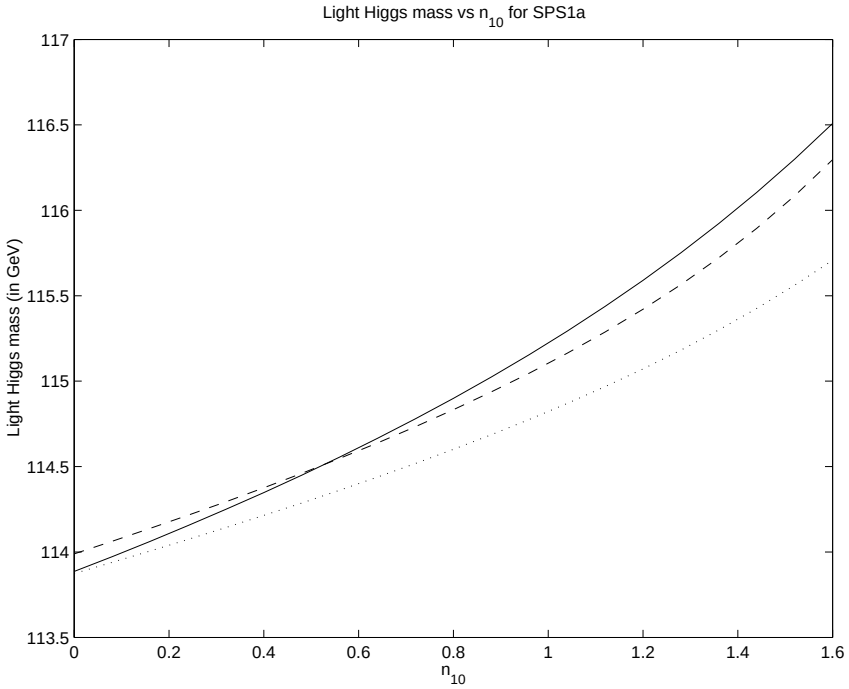

Fig.4: Plot of the light CP-even Higgs mass against n_{10} for SPS1a. Solid, dashed and dotted lines correspond to one, two and three-loop running respectively.

5. Conclusions

We have extended typical detailed running coupling analyses for the MSUGRA MSSM SPS benchmark points to incorporate three-loop β-function corrections for the running masses and couplings. We compare our results to those obtained by existing programs using two-loop running. The spread in the results from these programs is probably due to a mixture of program errors and genuine theoretical uncertainties such as the choice of scale appropriate for the evaluation of the pole mass. Presumably over time the results used by these programs will converge; we would argue that a more reliable estimate of the ultimate theoretical error in these spectrum calculations is currently provided by the difference between our two and three-loop calculations, as opposed to the spread in the various available two-loop results.

Generally speaking the effect of the three-loop running corrections is small for weakly-interacting particles but larger for the squark masses. For the light stop mass at the SPS5 point, we see an 8% effect, but more typically the effect is between 1% and 2%. This appears to us to represent a fundamental limit on the theoretical precision of squark mass theoretical predictions.

Finally we show how additional matter in SU_5 multiplets can affect the sparticle spectrum; more dramatically as the "semi-perturbative unification" regime [12] is approached.

Acknowledgements

DRTJ was supported by a PPARC Senior Fellowship, and a CERN Research Associate-ship, and was visiting CERN while most of this work was done. AK was supported by an Iranian Government Studentship. We thank Ben Allanach, Jon Bagger, Ruth Browne, John Gracey, Tilman Plehn and Graham Ross for conversations.

References

[1] I. Jack and D.R.T. Jones Phys. Lett. **B**415 (1997) 383

[2] I. Jack, D.R.T. Jones and A. Pickering, Phys. Lett. **B**432 (1997) 114

[3] L.V. Avdeev, D.I. Kazakov and I.N. Kondrashuk, Nucl. Phys. **B**510 (1998) 289

[4] I. Jack, D.R.T. Jones and C.G. North, Nucl. Phys. **B**473 (1996) 308

[5] I. Jack, D.R.T. Jones and C.G. North, Nucl. Phys. **B**486 (1997) 479

[6] P.M. Ferreira, I. Jack and D.R.T. Jones, Phys. Lett. **B**387 (1996) 80

[7] http//www.liv.ac.uk/∼dij/betas

[8] B.C. Allanach *et al.*, Eur. Phys. J. **C** 25 (2002) 113

[9] http://kraml.home.cern.ch/kraml/comparison

[10] B.C. Allanach, S. Kraml and W. Porod, JHEP 016 (2003) 0303

[11] N. Ghodbane and H.U. Martyn, hep-ph/0201233.

[12] C.F. Kolda and J. March-Russell, Phys. Rev. **D**55 (1997) 4252

[13] D. Ghilencea, M. Lanzagorta and G.G. Ross, Phys. Lett. **B**415 (1997) 253 ; Nucl. Phys. **B**511 (1998) 3;
G. Amelino-Camelia, D. Ghilencea and G.G. Ross, Nucl. Phys. **B**528 (1998) 35

[14] B. Brahmachari, U. Sarkar and K. Sridhar, Mod. Phys. Lett. A **8** (1993) 3349;
R. Hempfling, Phys. Lett. **B**351 (1995) 206;
K.S. Babu and J.C. Pati, Phys. Lett. **B**384 (1996) 140

[15] I. Jack, D.R.T. Jones and A.F. Kord, Phys. Lett. **B**579 (2004) 180

[16] I. Jack, D.R.T. Jones and R. Wild, Phys. Lett. **B**509 131 (2001)

[17] I. Jack, D.R.T Jones, S.P. Martin, M.T. Vaughn and Y. Yamada, Phys. Rev. D **50**, 5481 (1994)

[18] D.R.T. Jones, Phys. Lett. **B**123 (1983) 45 ;
V. Novikov et al, Nucl. Phys. **B**229 (1983) 381 ;
V. Novikov et al, Phys. Lett. **B**166 (1986) 329 ;
M. Shifman and A. Vainstein, Nucl. Phys. **B**277 (1986) 456

[19] I. Jack, D.R.T. Jones and A. Pickering, Phys. Lett. **B**432 (1998) 114

[20] W. Siegel, Phys. Lett. **B**84 (1979) 193;
D.M. Capper, D.R.T. Jones and P. van Nieuwenhuizen, Nucl. Phys. **B**167 (1980) 479

[21] J.E. Björkman and D.R.T. Jones, Nucl. Phys. **B**259 (1985) 533

[22] D.I. Kazakov, hep-ph/0208200

[23] I. Jack and D.R.T. Jones, Phys. Lett. **B**473 (2000) 102;
I. Jack, D.R.T. Jones and S. Parsons, Phys. Rev. **D**62 (2000) 125022;
I. Jack and D.R.T. Jones, Phys. Rev. **D**63 (2001) 075010

[24] D.M. Pierce, J.A. Bagger, K.T. Matchev and R.J. Zhang, Nucl. Phys. **B**491 (1997) 3

[25] J.L. Feng, K.T. Matchev and T. Moroi, Phys. Rev. **D**61 (2000) 075005